

Equal-Chord Attitude Determination Method for Spinning Spacecraft

Jozef C. van der Ha*

Spacecraft Design and Operations, Columbia, Maryland 21044

The equal-chord method offers a straightforward and low-cost technique for the determination of the spin-axis attitude using sun and Earth sensor data. The Earth aspect angle follows from the time at which the chord lengths measured by the Earth sensor's two pencil beams are equal. An estimation technique is not required, but linear or quadratic fitting of the sensor data should be performed to remove the random errors. The accuracy of the attitude solution obtained by the equal-chord method in the presence of the relevant biases is evaluated. The result is insensitive to uniform biases in the measured chord angles, caused for instance by errors in the Earth's infrared horizon. Finally, the application of the method is demonstrated using actual flight data of the CONTOUR spacecraft.

I. Introduction

SPIN stabilization is an attractive means for providing spacecraft pointing stability during injection maneuvers performed for instance by means of a solid rocket motor (SRM). This concept is used when injecting geostationary spacecraft from their transfer orbits into their planned stationary orbits. The same approach can also be employed^{1,2} for the injection of a probe into a deep-space trajectory as was done in the case of the Comet Nucleus Tour (CONTOUR) mission in August 2002. Because errors in the resulting trajectory must be corrected afterwards at the expense of precious onboard fuel, it is imperative^{2,3} that the error in the injection attitude should be as small as possible: typical requirements are in the range from 0.5 to 1.0 deg.

For the purpose of attitude determination, we need knowledge of the attitude orientation with respect to known inertial reference directions. In the CONTOUR case the integrated Earth–sun sensor of Galileo Avionica produces angular measurements of the spin axis relative to the sun and Earth directions.^{3,4} The CONTOUR Earth sensor is equipped with two pencil beams scanning the Earth over different paths. The crossing times of the Earth's infrared horizon during the scans produce two independent chord-angle and sun–Earth dihedral-angle measurements.

There exists a great deal of literature on the determination of the attitude pointing of a spinning spacecraft (see Wertz⁵). The determination of the spin-axis attitude is usually performed by means of an estimation technique (e.g., weighted least squares) using a batch of downlinked sensor measurements. The accuracy of the resulting attitude solution will be influenced by random as well as systematic errors (i.e., biases). The influence of random noise can easily be removed by employing a sufficiently large set of measurement data. The adverse effects of biases, however, cannot be mitigated in a straightforward manner so that the accuracy of the attitude solution is often tainted by the presence of appreciable (but unknown) biases.

The present paper describes the so-called equal-chord method, which performs a spin-axis attitude determination on the basis of the sensor measurements referred to a single point during the Earth-sensor coverage interval. This point corresponds to the time at which

the chord angles measured by the two pencil beams of the Earth sensor are exactly equal (this occurs when the two chords are symmetrical with respect to the Earth's center). Applicable spacecraft typically have two (or more) pencil beams, each having its own coverage interval during which the cone formed by its scanning motion intersects the Earth. The location of the coverage interval within the orbit is determined by the spin-axis pointing direction and by the specific mounting orientation of the pencil beam. The existence of the point of equal chords can be guaranteed if the coverage intervals of the two pencil beams are partly overlapping along the spacecraft orbit. This condition is in fact fulfilled by virtually all applicable spacecraft.

The instantaneous Earth aspect angle (i.e., the angle between the spin-axis orientation and the spacecraft–Earth direction) follows immediately from the time of equal chords or can also be derived from the measured equal-chord angle. The spin-axis pointing direction is found by a straightforward single-frame geometric attitude-determination technique based on the sun aspect angle, the Earth aspect angle, and the sun–Earth dihedral angle at the time of equal chords.

The implementation of the equal-chord method is very undemanding in terms of software requirements and does not need a priori attitude knowledge. Fagg and van Holtz⁶ point out that the method provides an opportunity for in-flight calibration of the Earth sensor. In fact, the resulting attitude solution is insensitive to uniform biases in the chord measurements. As a consequence, uniform biases in the Earth's infrared radius have no appreciable influence on the result delivered by the equal-chord method. This is an attractive feature in practical spacecraft applications because the precision of infrared horizon models is inadequate for predicting Earth sensor crossing times as a result of unforeseeable variations caused by diurnal and local weather effects (Wertz,⁵ pp. 90–97).

The paper provides a detailed derivation of the measurement model underlying the equal-chord method. Furthermore, the effects of the relevant biases encountered in practice (e.g., errors in the Earth's infrared radiation profile and sensor mounting misalignments) on the attitude solution are analyzed in full detail. The application of the method is illustrated using the actual sensor measurements delivered by the CONTOUR spacecraft in August 2002.

II. Sensor Measurement Characteristics

A. Sensor Operating Principles

The sun sensor produces pulses at the instants when the sun passes over the meridian and skew slits (Fig. 1a), and these can readily be transformed into measurements of the sun aspect angle. The Earth sensor has two static pencil beams mounted at angles μ_i ($i = 1, 2$) relative to the spacecraft spin axis (CONTOUR

Presented as AAS Paper 2004-145 at the AAS/AIAA 14th Space Flight Mechanics Meeting, Maui, HI, 8–12 February 2004; received 5 May 2004; revision received 6 August 2004; accepted for publication 1 November 2004. Copyright © 2004 by the American Institute of Aeronautics and Astronautics, Inc. All rights reserved. Copies of this paper may be made for personal or internal use, on condition that the copier pay the \$10.00 per-copy fee to the Copyright Clearance Center, Inc., 222 Rosewood Drive, Danvers, MA 01923; include the code 0731-5090/05 \$10.00 in correspondence with the CCC.

*Consultant; jvdha@aol.com. Senior Member AIAA.

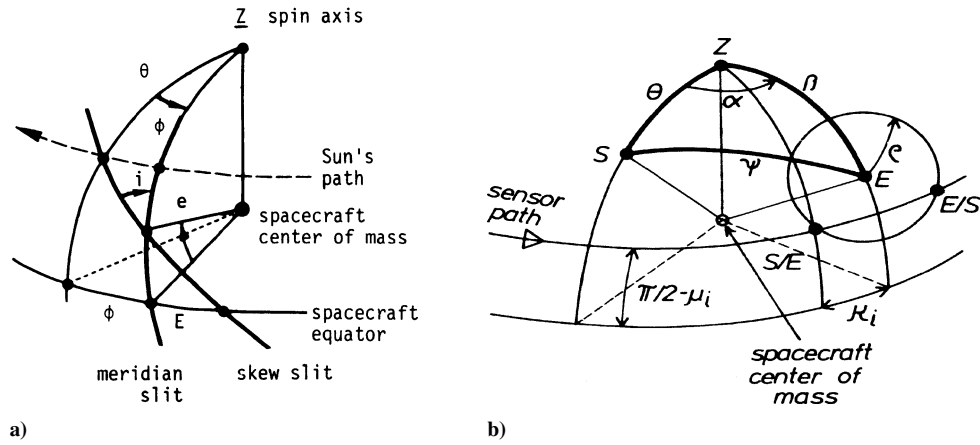


Fig. 1 Measurement principles for sun sensor and Earth sensor.

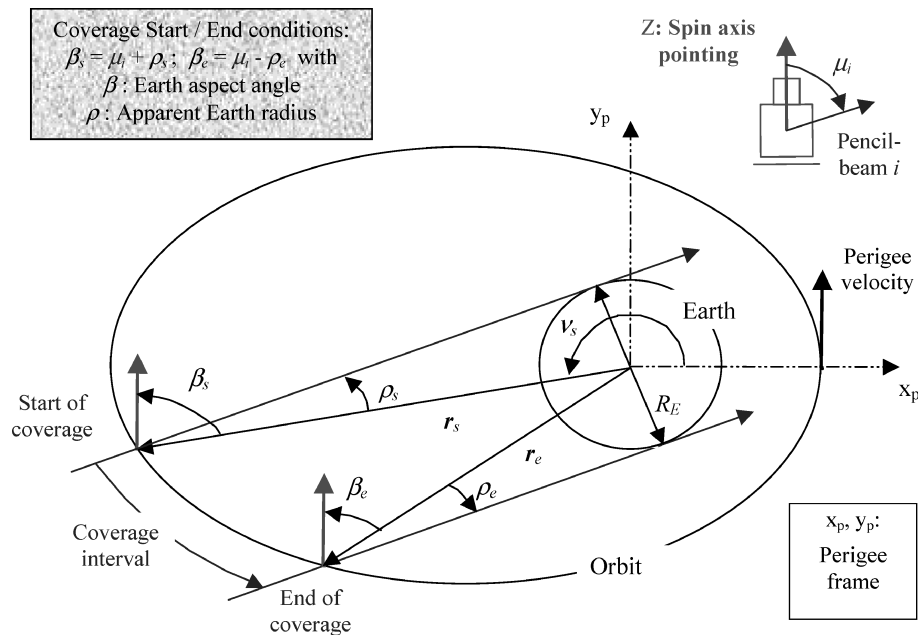


Fig. 2 Earth sensor pencil-beam coverage interval (projected view).

has $\mu_1 = 60$ and $\mu_2 = 65$ deg). The sensor produces measurements of the space/Earth and Earth/space crossing times of the Earth's infrared horizon (Fig. 1b). These crossings determine the half-chord angles κ_i (one for each of the pencil beams $i = 1, 2$). When combining the Earth sensor crossings with the sun sensor's meridian slit crossing time, we obtain two measurements α_i of the sun–Earth dihedral angle. This angle is formed (Fig. 1b) when the spacecraft rotates about its Z axis from the meridian containing the sun vector up to the meridian containing the center of the Earth's disk.

The design of the CONTOUR Earth sensor was customized for the CONTOUR-specific phasing orbits² with perigee altitudes near 200 km and apogees of about 115,000 km. The sensor delivers its best performance over the altitude range from about 50,000 to 60,000 km, which matches the Earth sensor coverage intervals for the nominal CONTOUR SRM injection attitude. The specific CONTOUR pencil-beam settings place the sensor coverage intervals after the apogees of the phasing orbits (Fig. 2).

B. Earth Sensor Measurements

Figure 3 shows the evolution of the measured half-chord angles κ_i (for the two pencil beams $i = 1, 2$) as a function of the Earth aspect

angle β for the nominal CONTOUR conditions. The half-chord angles κ_i satisfy the geometrical measurement equations [Wertz,⁵ Eqs. (11-7) and (11-8)]:

$$\cos \mu_i \cos \beta + \sin \mu_i \sin \beta \cos \kappa_i = \cos \rho(v) \quad (i = 1, 2) \quad (1)$$

The half-chord angles in Fig. 3 were generated from Eqs. (1) using an a priori known spin-axis attitude direction with unit vector Z . On account of the relation $\beta(v) = \arccos \{Z \cdot E(v)\}$, the Earth aspect angle β will be known (during simulations) as a function of the true anomaly v and other orbital elements. [Note: the spacecraft-to-Earth unit-vector $E(v)$ is defined by $-r(v)/r(v)$ and points in the opposite direction of the orbital position vector r .]

The angle $\rho(v)$ is the apparent Earth radius angle seen by the Earth sensor from the instantaneous orbital true anomaly position v (Fig. 2). The nominal evolution of $\rho(v)$ is shown in Fig. 3 and follows from the knowledge of the orbital elements:

$$\rho(v) = \arcsin \{R_E/r(v)\} \quad \text{with} \quad r(v) = \ell / (1 + e \cos v) \quad (2)$$

The orbital elements ℓ and e denote the semilatus rectum and the eccentricity, respectively. The orbital radius $r(v)$ is usually known fairly accurately (i.e., the error Δr is below 1 km), and so the error $\Delta \rho_r = -(\Delta r/r) \tan \rho$ remains below 0.001 deg within the coverage interval and is thus negligible.

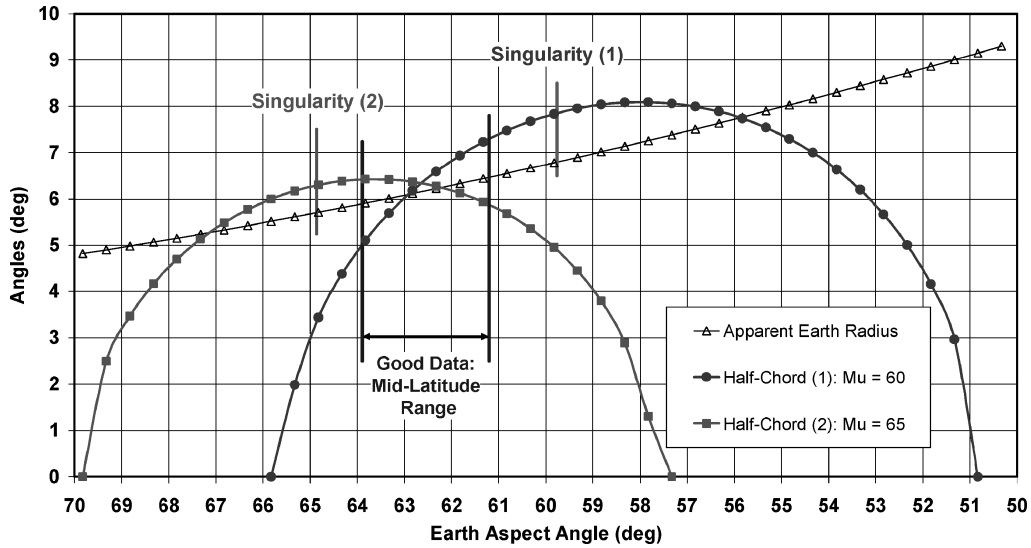


Fig. 3 Half-chord angles and apparent Earth radius vs Earth aspect angle.

The radius R_E in Eq. (2) stands for the Earth's infrared radius observed by the Earth sensor. The extent of the Earth's mean infrared radiance profile (in the CO_2 spectral band) reaches to about 40 km above the Earth's surface (Wertz,⁵ pp. 90–97). Because the mean radius of the solid Earth is about 6367.5 km, it follows that the mean infrared Earth radius is $R_E \cong 6407.5$ km. This corresponds to the “effective” horizon for the Earth sensor, which is designed to trigger at 50% of the observed peak radiance. The uncertainty in the triggering altitude is hard to predict, but 5 km ($1\text{-}\sigma$ level) should be conservative.

It must be kept in mind that each of the two pencil beams can come across a different Earth radius because of (a priori unknown) temporal and local variations in the Earth's infrared profiles at the locations where the pencil beams have their in- and out-crossings. Another error source that comes into play is induced by the Earth's oblateness. The scan paths of the pencil beams can cross the Earth's rim at about any location (with different probability densities). For simplicity we assume that errors caused by oblateness can be modeled by a Gaussian distribution with an uncertainty of 4 km ($1\text{-}\sigma$ level). The combination of the two (independent) error sources affecting the sensor triggering altitude amounts to 6.4 km (1σ). The error in the apparent Earth radius $\Delta\rho_E \cong (\Delta R_E/r)$ will be less than 0.01 deg in the CONTOUR case and about twice as high for geostationary transfer orbits.

C. Calculation of Earth Aspect Angle

During in-flight operations, the half-chord angles $\kappa_i(\nu)$ shown in Fig. 3 represent the fundamental measurements from which the unknown Earth aspect angle should be determined. Equations (1) indicate that each of the two chord-angle measurements κ_i ($i = 1, 2$) produces its own solution β_i . This solution can be written in a form that shows the explicit dependency of the Earth aspect angle $\beta_i(\nu)$ on the corresponding half-chord measurement $\kappa_i(\nu)$ at the time $t(\nu)$:

$$\beta_i(\nu) = \tan^{-1} \left\{ \tan \mu_i \cos \kappa_i(\nu) \right\} \\ \pm \cos^{-1} \left\{ \frac{\cos \rho(\nu)}{\left[1 - \sin^2 \mu_i \sin^2 \kappa_i(\nu) \right]^{\frac{1}{2}}} \right\} \quad (i = 1, 2) \quad (3)$$

This result shows that there is (in general) a two-fold ambiguity in the calculation of the Earth aspect angle β_i from a given half-chord measurement κ_i . (This is evident from Fig. 3.) The selection of the appropriate sign for the solution β_i can usually be decided through a priori knowledge. A single optimal solution $\beta^*(\nu)$ can be constructed by weighting the individual $\beta_i(\nu)$ ($i = 1, 2$) on the

basis of their individual error covariances (as shown in previous papers^{3,7}).

The usefulness of the Earth sensor data usually varies significantly during the sensor coverage intervals in accordance with the lengths of the measured chords and the changing geometrical sensitivity conditions. Therefore, the data interval to be processed should be selected with care. The midlatitude region indicated in Fig. 3 provides the most valuable chord measurements for both pencil beams under the CONTOUR conditions.

D. Error Propagation Model

Equations (1) and (3) make use of the ideal apparent Earth radius $\rho(\nu)$, which is independent of the actual attitude and of the sensor measurements. In practice, however, the actual Earth radii ρ_i at a given time and location will likely differ from the expected ideal value and might also be different for the two pencil beams. Because the actual values are unknown, operational attitude-determination algorithms must employ the nominal evolution $\rho(\nu)$ of Eq. (2) in the calculation of the Earth aspect angle β_i from the measured half-chord angles κ_i . The establishment of a model for the propagation of the actual errors $\Delta\rho_i$ in the Earth radii ρ_i ($i = 1, 2$) is fairly intricate. For practical applications we advocate an approach that models the errors $\Delta\rho_i$ in terms of their effects on the resulting chord measurements. Subsequently, the propagation of $\Delta\kappa_i$ errors into the resulting Earth aspect angle β_i can be calculated on the basis of the ideal error-free evolution of $\rho(\nu)$.

An error $\Delta\rho_i$ induces a change $\Delta\kappa_i$ in the half-chord-angle measurement κ_i in accordance with the sensitivity function $\partial\kappa_i/\partial\rho_i$ that follows from Eq. (1):

$$\Delta\kappa_i = \left(\frac{\partial\kappa_i}{\partial\rho_i} \right) \Delta\rho_i = \left\{ \frac{\sin \rho(\nu)}{\sin \mu_i \sin \beta \sin \kappa_i} \right\} \Delta\rho_i \quad (i = 1, 2) \quad (4)$$

The sensitivity function $\partial\beta_i/\partial\kappa_i$ can also be found from Eq. (1) and expresses the variation of the Earth aspect angle β_i induced by the error $\Delta\kappa_i$ in the half-chord angles:

$$\Delta\beta_i = \left(\frac{\partial\beta_i}{\partial\kappa_i} \right) \Delta\kappa_i = \left\{ \frac{\sin \mu_i \sin \beta \sin \kappa_i}{(\sin \mu_i \cos \beta \cos \kappa_i - \cos \mu_i \sin \beta)} \right\} \Delta\kappa_i \\ (i = 1, 2) \quad (5)$$

By multiplying the results of Eqs. (4) and (5), we obtain the error $\Delta\beta_i$ resulting from the error $\Delta\rho_i$ in the local apparent Earth radius ρ_i as propagated by the measured half-chord angle κ_i . It

Table 1 Summary of relationships at singularity points ($i = 1, 2$)

Relationship	Inverse relationship	CONTOUR values
$\beta_{i,s}(\kappa_{i,s}) = \tan^{-1}\{\tan \mu_i \cos \kappa_{i,s}\}$	$\kappa_{i,s}(\beta_{i,s}) = \cos^{-1}\{\tan \beta_{i,s} / \tan \mu_i\}$	$\kappa_{1,s} = 7.855$ deg; $\kappa_{2,s} = 6.293$ deg
$\beta_{i,s}(\rho_{i,s}) = \cos^{-1}\{\cos \mu_i / \cos \rho_{i,s}\}$	$\rho_{i,s}(\beta_{i,s}) = \cos^{-1}\{\cos \mu_i / \cos \beta_{i,s}\}$	$\beta_{1,s} = 59.766$ deg; $\beta_{2,s} = 64.867$ deg
$\rho_{i,s}(\kappa_{i,s}) = \sin^{-1}\{\sin \mu_i \sin \kappa_{i,s}\}$	$\kappa_{i,s}(\rho_{i,s}) = \sin^{-1}\{\sin \rho_{i,s} / \sin \mu_i\}$	$\rho_{1,s} = 6.797$ deg; $\rho_{2,s} = 5.702$ deg

is obvious that Eq. (5) also describes the propagation of (sensor-internal) measurement errors $\Delta\kappa_i$ that have not been induced by $\Delta\rho_i$ errors.

E. Measurement Singularities

The denominator of Eq. (5) vanishes at the singular points (see Fig. 3) defined by the Earth aspect angle $\beta_{i,s} = \beta_i(v_s)$:

$$\beta_{i,s} = \tan^{-1}\{\tan \mu_i \cos \kappa_{i,s}\} \quad (i = 1, 2) \quad (6)$$

When checking back with Eq. (3), we find that the singularity corresponds to the point in the coverage interval where the Earth aspect angle has just one solution associated with the measured chord angle. It is also evident from Eq. (3) that the half-chord angle at the singularity point will be equal to $\kappa_{i,s} = \sin^{-1}\{\sin \rho_{i,s} / \sin \mu_i\}$ with $\rho_{i,s} = \rho_i(v_s)$ for each of the pencil beams $i = 1, 2$.

At the singular point, the sensitivity of the Earth aspect-angle determination to the relevant errors in the chord angle is most unfavorable. In mathematical terms, the singularity amounts to a zero-measurement-density case and corresponds to the scan near the middle of the Earth's disk [see also Wertz,⁵ p. 386, below Eq. (11-40)]. It should be noted that the points $\beta_{i,s}$ and $\kappa_{i,s}$ do in general not coincide with the location of the maximum chord over the coverage interval. The increasing apparent Earth radius shifts the actual maximum away to a lower value of the Earth aspect angle as can be observed in Fig. 3.

Figure 3 illustrates that the point of equal chords is far away from the singularities of the two pencil beams so that the individual measurement characteristics of the two chords are relatively favorable at this point.

Table 1 summarizes all possible relationships between $\beta_{i,s}$, $\kappa_{i,s}$, and $\rho_{i,s}$ as well as the nominal values for CONTOUR at the singularity points for the two pencil beams.

III. Equal-Chord Method

A. Summary of Procedure

The equal-chord attitude-determination method uses the angular measurements referred to just one particular time t_e (and true anomaly v_e), namely, when the lengths of the chords scanned by the two pencil beams are precisely equal. The specific instant t_e at which the chords become equal is determined by the actual spin-axis attitude orientation, by the sensor mounting angles, and by the orbital characteristics. The length of the equal half-chord at time t_e will be denoted by $\kappa_e = \kappa_1(t_e) = \kappa_2(t_e)$.

The core of the method consists of the calculation of the Earth aspect angle β_e from the measured half-chord angle κ_e or from the time t_e at which the chords are equal. The measurements κ_e and t_e should be extracted from the noisy Earth sensor measurements by processing an interval of telemetry data centered on an a priori predicted equal-chord time. The measured time of equal chords t_e is identified as the instant when the quadratic approximations of the two arcs of half-chord measurements $\kappa_i(t)$ intersect to become κ_e . About 1000 data points (i.e., about 17 min of sensor measurements at 60 rpm spin rate) will be sufficient to reduce the influence of the random errors to insignificance.

Finally, we employ a single-frame geometric attitude-determination method on the basis of the sun and Earth aspect-angle measurements ϑ_e and β_e . For enhancement of the accuracy of the attitude solution, also the sun–Earth dihedral angle α_e at the equal-chord time should be used. The angles $\vartheta(t)$ and $\alpha(t)$ vary much more slowly than the chord angles so that ϑ_e and α_e can be established by a linear fitting procedure centered on the equal-chord time

t_e . The knowledge of t_e provides the relevant orbital elements and the reference sun and Earth vectors that are used in the attitude-determination procedure.

The operational application of the equal-chord method offers significant advantages when compared with other batch attitude estimation methods (e.g., least squares). After the straightforward linear and quadratic fitting of the raw measurement angles, the equal-chord method employs only one set of measurement data referred to one known instant of time t_e . The attitude solution follows from the inversion of the single-frame measurement equations involving ϑ_e , β_e , and α_e . The least-squares method, on the other hand, processes the complete batch of data (typically consisting of about 1000 instants of sensor data). Each of the data points in the batch has its own set of measurement equations with different coefficients (because of the varying Earth position). The attitude estimate is found by means of the pseudoinverse algorithm (Wertz,⁵ p. 749) involving the multiplication of a number of very large matrices. If a sequential filtering technique (e.g., Kalman filter) were to be used, the large matrices will be avoided, but even in this case each of the points in the large batch of data must be processed individually.

B. Nominal Equal-Chord Model

First, we establish the nominal equal-chord model, which refers to the ideal situation when measurement biases are absent. The condition that the chords produced by the two pencil beams are equal at the time t_e can be formulated as

$$\kappa_e = \kappa_1(\beta_e, \rho_e, \mu_1) = \kappa_2(\beta_e, \rho_e, \mu_2) \quad (7)$$

The Earth aspect angle and the apparent Earth radius angle appearing here should obviously be interpreted as $\beta_e = \beta(v_e)$ and $\rho_e = \rho(v_e)$ with $v_e = v(t_e)$ denoting the true anomaly at the equal-chord time t_e .

The objective of the following analysis is to express the Earth aspect angle β_e in terms of the measured half-chord angle κ_e or in terms of the known ρ_e (at the measured equal-chord time t_e). We consider the two chord equations in Eq. (1) at the time of equal chords t_e and write them in the matrix form:

$$\begin{bmatrix} \cos \mu_1 & \sin \mu_1 \\ \cos \mu_2 & \sin \mu_2 \end{bmatrix} \begin{pmatrix} \cos \beta_e \\ \sin \beta_e \cos \kappa_e \end{pmatrix} = \begin{pmatrix} \cos \rho_e \\ \cos \rho_e \end{pmatrix} \quad (8)$$

It will be convenient to introduce the sensor mounting matrix $[\mu]$ defined by

$$[\mu] = \begin{bmatrix} \cos \mu_1 & \sin \mu_1 \\ \cos \mu_2 & \sin \mu_2 \end{bmatrix} \quad (9)$$

Its inverse matrix $[\mu]^{-1}$ is given by

$$[\mu]^{-1} = \frac{1}{2} \begin{bmatrix} c_\mu + s_\mu & c_\mu - s_\mu \\ f_\mu - g_\mu & f_\mu + g_\mu \end{bmatrix} \quad (10)$$

with

$$\begin{aligned} c_\mu &= \cos \mu / (\cos d), & s_\mu &= \sin \mu / (\sin d) \\ f_\mu &= \sin \mu / (\cos d), & g_\mu &= \cos \mu / (\sin d) \end{aligned} \quad (11)$$

The parameter $\mu = \frac{1}{2}(\mu_2 + \mu_1)$ denotes the mean value of the two pencil-beam mounting angles, and $d = \frac{1}{2}(\mu_2 - \mu_1)$ represents half

Table 2 Summary of relationships at instant of equal chords

Relationship	Inverse relationship	CONTOUR values
$\beta_e(\kappa_e) = \tan^{-1}\{\tan \mu / \cos \kappa_e\}$	$\kappa_e(\beta_e) = \cos^{-1}\{\tan \mu / \tan \beta_e\}$	$\kappa_e \cong 6.339$ deg
$\beta_e(\rho_e) = \cos^{-1}\{c_\mu \cos \rho_e\}$	$\rho_e(\beta_e) = \cos^{-1}\{\cos \beta_e / c_\mu\}$	$\beta_e \cong 62.644$ deg
$\rho_e(\kappa_e) = \cos^{-1}\{\cos[\beta_e(\kappa_e)] / c_\mu\}$	$\kappa_e(\rho_e) = \cos^{-1}\{\tan \mu / \tan[\beta_e(\rho_e)]\}$	$\rho_e \cong 6.156$ deg

of the difference between these angles. With the help of these definitions, we can invert Eq. (8):

$$\begin{pmatrix} \cos \beta_e \\ \sin \beta_e \cos \kappa_e \end{pmatrix} = [\mu]^{-1} \begin{pmatrix} \cos \rho_e \\ \cos \rho_e \end{pmatrix} = \cos \rho_e \begin{pmatrix} c_\mu \\ f_\mu \end{pmatrix} \quad (12)$$

The two rows of Eq. (12) produce the following explicit results for $\beta_e(\rho_e)$ and $\kappa_e(\rho_e)$:

$$\beta_e(\rho_e) = \cos^{-1}\{c_\mu \cos \rho_e\}, \quad \kappa_e(\rho_e) = \cos^{-1}\left\{\frac{\tan \mu}{\tan[\beta_e(\rho_e)]}\right\} \quad (13)$$

These results express β_e and κ_e in terms of the known apparent Earth radius ρ_e at the time t_e .

Another important result is obtained by forming the quotient of the second and first rows of Eq. (12):

$$\tan \beta_e \cos \kappa_e = f_\mu / c_\mu = \tan \mu \rightarrow \beta_e(\kappa_e) = \tan^{-1}\{\tan \mu / \cos \kappa_e\} \quad (14)$$

The latter result provides β_e explicitly in terms of the measured κ_e angle. The relatively small value of κ_e (see Fig. 3) justifies the expansion of $\cos \kappa_e$ in Eq. (14):

$$\beta_e(\kappa_e) \cong \mu + \frac{1}{4}\kappa_e^2 \sin(2\mu) + \mathcal{O}(\kappa_e^4) \quad (15)$$

This expression illustrates that the Earth aspect angle at the time of equal chords will be close to the mean value of the sensor mounting angles. Figure 3 shows that $\kappa_e \cong 6.34$ deg for the CONTOUR design parameters (with $\mu = 62.5$ deg), and so we find $\beta_e \cong \mu + 0.144$ deg = 62.644 deg with an approximation error that is negligible when compared with the exact result of Eq. (14).

C. Interpretation of Equal-Chord Solution

The results in Eqs. (14) and (15) constitute the measurement equation for the calculation of the Earth aspect angle β_e from the measured equal-chord angle $\kappa_e = \kappa(t_e)$. An attractive feature of this approach is the fact that the sensitivity of β_e to errors in κ_e is practically negligible (e.g., $\partial\beta_e/\partial\kappa_e = 0.045$ in the case of CONTOUR). Therefore, bias errors in the measurement of the equal half-chord angle will have little effect on the resulting value of β_e . This result is in strong contrast with the sensitivity functions $\partial\beta_i/\partial\kappa_i$ of the two individual pencil beams with respective values of -1.75 and 2.30 at the time of equal chords. For completeness sake it should be noted, however, that the low sensitivity of β_e to errors in the measured κ_e angle by itself does not also imply a low attitude error. The biases can induce a shift in the time of equal chords so the Earth vector that forms the inertial reference for the attitude solution can change as well.

The first result in Eq. (13) offers an attractive alternative approach to the baseline equal-chord procedure just outlined. After the equal-chord time t_e has been extracted from the two sets of half-chord measurements $\kappa_i(t)$ for $i = 1, 2$, we can calculate the apparent Earth radius $\rho_e = \rho(v_e)$ from the available orbit information by means of Eq. (2). The expression for $\beta_e(\rho_e)$ in Eq. (13) provides now immediately the Earth aspect angle β_e . (Note: The measured equal-chord angle κ_e will not be used at all in this approach.) The relevant error sensitivity $\partial\beta_e/\partial\rho_e$ (i.e., 0.056 in the CONTOUR case) is similar in magnitude to that of $\partial\beta_e/\partial\kappa_e$ just given so that the approach based on ρ_e appears to be equivalent (in both practicality and error sensitivity) to the baseline equal-chord procedure using the measured κ_e .

D. Summary of Formulas

The equality condition for the two half-chord angles κ_i ($i = 1, 2$) in Eq. (7) leads to two equations for the three variables $\kappa_e, \beta_e, \rho_e$ with $\rho_e = \rho(t_e)$, a known function of t_e . Table 2 summarizes the six possible relationships between any two of these three variables as well as the specific CONTOUR equal-chord values. β_e lies close to midway between the singular points of the two chords (see Fig. 3 and Table 1), which demonstrates the favorable measurement characteristics of the equal-chord method.

E. Geometric Attitude Determination

The geometric attitude-determination procedure employs the Earth aspect angle β_e , the sun aspect angle ϑ_e , and (optionally) the sun–Earth dihedral angle α_e at the time of equal chords³:

$$\begin{aligned} \mathbf{Z} \cdot \mathbf{S}_e &= \cos \vartheta_e, & \mathbf{Z} \cdot \mathbf{E}_e &= \cos \beta_e \\ \mathbf{Z} \cdot (\mathbf{S}_e \times \mathbf{E}_e) &= \sin \vartheta_e \sin \beta_e \sin \alpha_e \end{aligned} \quad (16)$$

The angle α_e represents the mean value of the measurements $\alpha_i(t_e)$ obtained (after linear fits) from the individual pencil beams $i = 1, 2$. As long as the sun and Earth vectors \mathbf{S}_e and \mathbf{E}_e at the time t_e are not collinear, Eqs. (16) produce a unique attitude vector \mathbf{Z} (Shuster⁸). In geometrical terms, the first two equations produce two attitude solutions that correspond to the intersections of the two cones centered on the sun and Earth vectors \mathbf{S}_e and \mathbf{E}_e (with half-cone angles ϑ_e and β_e , respectively). The two-fold ambiguity in the attitude solution can be resolved by employing also the measurement α_e . Although the use of the α_e angle would typically enhance the accuracy of the resulting attitude solution, this can also introduce additional unknown bias effects.

The equal-chord method does not formally require an a priori attitude estimate, but some knowledge of the expected equal-chord time is needed for selecting the interval of telemetry data that should be processed. If this information is not available, we can find a rough estimate of t_e by visual inspection of a chart showing the downlinked chord measurements.

IV. Effects of Measurement Biases

A. New Equal-Chord Condition

The ideal equal-chord model just presented does not account for any bias errors that might affect the chord measurements. As mentioned already, the actual Earth radii for the two pencil beams can differ because of local and temporal variations in the Earth's infrared radiance profile. Also there might be sensor-internal errors caused (for instance) by limitations in the precision of the sensor calibration parameters. These biases introduce offsets $\Delta\kappa_i$ ($i = 1, 2$) in the measured half-chord angles, which can affect the resulting equal-chord measurement κ_e as well as the time of equal chords t_e . As a consequence, the Earth aspect angle found by the equal-chord calculations can differ from the ideal nominal result already established.

When accounting for the biases of the half-chord angles, we can rewrite the equal-chord condition in Eq. (7) in the form

$$\kappa_{e,\text{new}} = \kappa_1(\beta_{e,\text{new}}, \rho_{e,\text{new}}, \mu_1) + \Delta\kappa_1 = \kappa_2(\beta_{e,\text{new}}, \rho_{e,\text{new}}, \mu_2) + \Delta\kappa_2 \quad (17)$$

The new equal half-chord angle $\kappa_{e,\text{new}}$ will in general be different from the ideal κ_e because of the bias offsets $\Delta\kappa_i$ ($i = 1, 2$) in the equal-chord data. Because the biases are assumed “small,” the resulting shift $\Delta\kappa_e$ in the equal-chord angle $\kappa_{e,\text{new}}$ relative to κ_e can

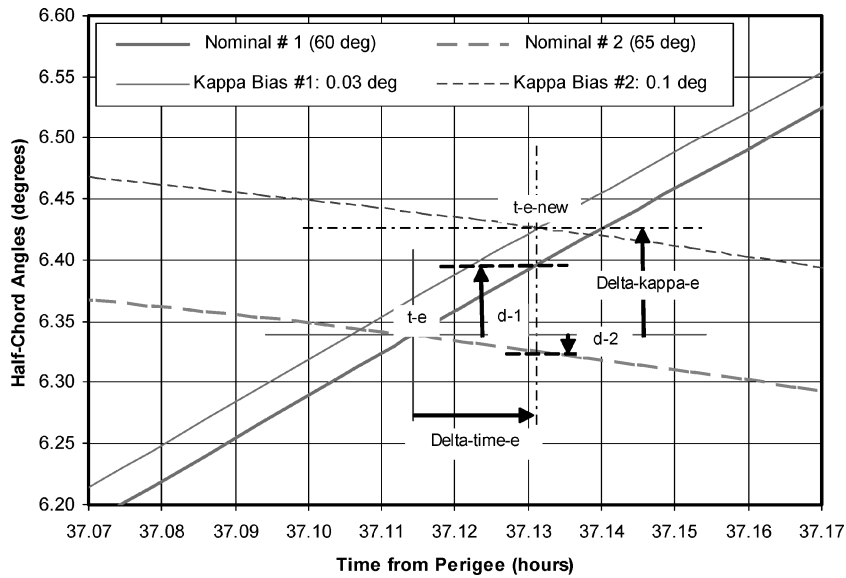


Fig. 4 Illustration of bias effects on equal-chord condition.

also be considered small, and the equal-chord condition (17) can be expressed as

$$\kappa_{e,\text{new}} = \kappa_i(\beta_{e,\text{new}}, \rho_{e,\text{new}}, \mu_i) + \Delta\kappa_i = \kappa_e + \Delta\kappa_e \quad (i = 1, 2) \quad (18)$$

Furthermore, the new angular variables $\rho_{e,\text{new}}$ and $\beta_{e,\text{new}}$ will also be close to their respective nominal equal-chord values ρ_e and β_e :

$$\rho_{e,\text{new}} = \rho_e + \Delta\rho_e, \quad \beta_{e,\text{new}} = \beta_e + \Delta\beta_e \quad (19)$$

with small changes $\Delta\rho_e$ and $\Delta\beta_e$.

In practical applications we have no advance knowledge on the presence and magnitude of the biases. Therefore, the calculation of $\beta_{e,\text{new}}$ from the equal-chord angle $\kappa_{e,\text{new}}$ or from the Earth radius $\rho_{e,\text{new}}$ at the new equal-chord time $t_{e,\text{new}}$ will be performed as in the nominal case described by Eqs. (13) and (14):

$$\beta_{e,\text{new}}(\rho_{e,\text{new}}) = \cos^{-1}\{c_\mu \cos \rho_{e,\text{new}}\}$$

$$\beta_{e,\text{new}}(\kappa_{e,\text{new}}) = \tan^{-1} \left\{ \frac{\tan \mu}{\cos \kappa_{e,\text{new}}} \right\} \quad (20)$$

After substituting the expressions from Eqs. (18) and (19) into Eq. (20) and performing expansions for small deviations from the nominal equal-chord solution, we find the variations in the resulting Earth aspect-angle solutions:

$$\Delta\beta_e \cong \{\tan \rho_e / \tan \beta_e\} \Delta\rho_e, \quad \Delta\beta_e \cong \frac{1}{2} \{\sin(2\beta_e) \tan \kappa_e\} \Delta\kappa_e \quad (21)$$

For the nominal CONTOUR parameters given in Table 2, we retrieve the favorable error sensitivity results (i.e., $\Delta\beta_e \cong 0.056\Delta\rho_e$ and $\Delta\beta_e \cong 0.045\Delta\kappa_e$) that were already mentioned.

B. Changes in Equal-Chord Measurements

Next, we seek to establish explicit expressions for the changes $\Delta\rho_e$ and $\Delta\kappa_e$ in the fundamental equal-chord measurements ρ_e and κ_e in terms of the biases $\Delta\kappa_i$ ($i = 1, 2$). It may be recalled that $\Delta\rho_e$ is related to Δt_e by means of $\Delta\rho_e \cong \dot{\rho}_e \Delta t_e$ with known $\dot{\rho}_e$ so that we can use t_e and Δt_e instead of ρ_e and $\Delta\rho_e$.

Because the biases are small, the difference $\Delta t_e = t_{e,\text{new}} - t_e$ between the new and the nominal equal-chord times can also be considered small. Therefore, it is meaningful to use the linear approximations of the individual half-chords $\kappa_i(t)$ near the nominal equal-chord value κ_e :

$$\kappa_1(t_{e,\text{new}}) \cong \kappa_e + \dot{\kappa}_{1,e} \Delta t_e, \quad \kappa_2(t_{e,\text{new}}) \cong \kappa_e + \dot{\kappa}_{2,e} \Delta t_e \quad (22)$$

The subscript e specifies that the partial derivatives are evaluated at the nominal equal-chord time t_e . The time derivatives of the chord angles $\kappa_i(t)$ in Eqs. (17) and (18) can be expressed as

$$\dot{\kappa}_{i,e} = \left(\frac{\partial \kappa_i}{\partial \beta} \right)_e \dot{\beta}_e + \left(\frac{\partial \kappa_i}{\partial \rho} \right)_e \dot{\rho}_e \quad (i = 1, 2) \quad (23)$$

The calculation of the partials $(\partial \kappa_i / \partial \beta)_e$ and $(\partial \kappa_i / \partial \rho)_e$ is relatively straightforward and the results are similar to those in Eqs. (4) and (5). During simulations, the attitude will be known so that we can evaluate the derivative $\dot{\beta}_e$ at the time t_e . Therefore, $\dot{\kappa}_{i,e}$ in Eq. (23) can be calculated explicitly, and the changes d_i in the individual chords over the interval of time Δt_e (see Fig. 4) are found to be

$$d_i = \kappa_i(t_{e,\text{new}}) - \kappa_e \cong \dot{\kappa}_{i,e} \Delta t_e \quad (i = 1, 2) \quad (24)$$

The new equal-chord conditions given in Eq. (18) can be reformulated as

$$d_i + \Delta\kappa_i = \Delta\kappa_e \rightarrow \begin{bmatrix} 1 & -\dot{\kappa}_{1,e} \\ 1 & -\dot{\kappa}_{2,e} \end{bmatrix} \begin{pmatrix} \Delta\kappa_e \\ \Delta t_e \end{pmatrix} = \begin{pmatrix} \Delta\kappa_1 \\ \Delta\kappa_2 \end{pmatrix} \quad (25)$$

After inversion we find the explicit results for $\Delta\kappa_e$ and Δt_e in terms of the biases $\Delta\kappa_i$ ($i = 1, 2$):

$$\begin{pmatrix} \Delta\kappa_e \\ \Delta t_e \end{pmatrix} = \{\dot{\kappa}_{2,e} - \dot{\kappa}_{1,e}\}^{-1} \begin{bmatrix} \dot{\kappa}_{2,e} & -\dot{\kappa}_{1,e} \\ 1 & -1 \end{bmatrix} \begin{pmatrix} \Delta\kappa_1 \\ \Delta\kappa_2 \end{pmatrix} \quad (26)$$

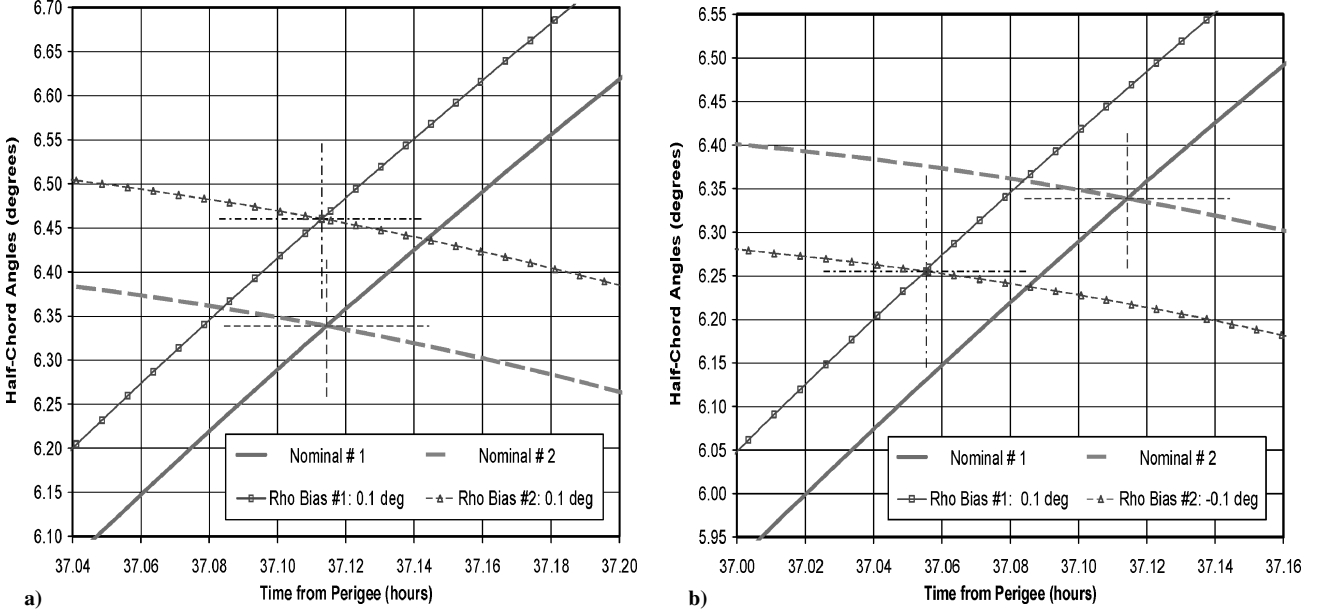
C. Discussion of Results

Figure 4 illustrates the shift Δt_e in the time of equal chords and the change $\Delta\kappa_e$ in the equal half-chord angle for an example with selected biases $\Delta\kappa_1 = 0.03$ deg and $\Delta\kappa_2 = 0.10$ deg. Relations (24) produce the individual changes $d_1 = 0.0573$ deg and $d_2 = -0.0127$ deg in the new equal chord $\kappa_{e,\text{new}}$ with respect to the original equal-chord angle κ_e . The shifts in the equal-chord measurements follow from Eqs. (26): $\Delta t_e = 0.0169$ h (or $\Delta\rho_e = 0.0146$ deg) and $\Delta\kappa_e = 0.0873$ deg. With the help of Eqs. (21), we find the changes in the Earth aspect angle produced by each of the two equal-chord approaches: $\Delta\beta_e(\Delta\rho_e) \cong 0.0008$ deg and $\Delta\beta_e(\Delta\kappa_e) \cong 0.0040$ deg. The difference between the two results is caused by the characteristics of the biases in terms of their effects on either κ_e or ρ_e . The change in the resulting Earth aspect angle is relatively small in comparison to the magnitude of the biases, which confirms the low error sensitivity of the equal-chord method.

Table 3 presents the results of simulations based on the CONTOUR conditions. The last two columns provide the changes

Table 3 Effects of measurement biases on resulting attitude solution

Input biases	Changes in equal-chord parameters				Change in attitude	
	Δt_e , h	$\Delta \kappa_e$, deg	$\Delta \beta_e(\Delta \rho_e)$, deg	$\Delta \beta_e(\Delta \kappa_e)$, deg	$(\Delta \rho_e)$, deg	$(\Delta \kappa_e)$, deg
Identical: $\Delta \kappa_1 = \Delta \kappa_2 = 0.1$ deg	0	0.1	0	0.00457	0	0.0033
Opposite: $\Delta \kappa_1 = -\Delta \kappa_2 = 0.1$ deg	-0.04810	-0.06892	-0.00229	-0.00311	0.1423	0.1429
Chord # 1 only: $\Delta \kappa_1 = 0.1$ deg; $\Delta \kappa_2 = 0$	-0.02409	0.01649	-0.00116	0.00075	0.0715	0.0701
Chord # 2 only: $\Delta \kappa_1 = 0$; $\Delta \kappa_2 = 0.1$ deg	-0.02415	0.08155	0.00117	0.00372	0.0720	0.0738
Uniform R_E : $\Delta \rho_1 = \Delta \rho_2 = 0.1$ deg	-0.00135	0.12164	-0.00007	0.00557	0.0040	0
Opposite R_E : $\Delta \rho_1 = -\Delta \rho_2 = 0.1$ deg	-0.05933	-0.08338	-0.00282	-0.00376	0.1754	0.1761

**Fig. 5** Geometry of chords near point of equal chords under $\Delta \rho$ biases.

in the attitude solutions caused by the biases as predicted by each of the two equal-chord approaches. In the first row of Table 3, both biases are equal to $+0.1$ deg, and so there will be no shift in the time of equal chords (because $\kappa_e + \Delta \kappa_1$ equals $\kappa_e + \Delta \kappa_2$ at t_e), which is correctly predicted by the second row of Eq. (26). The first formula in Eq. (21), which is based on $\Delta \rho_e$, predicts that there will also be no change in the resulting $\Delta \beta_e$. The second formula, on the other hand, uses $\Delta \kappa_e$ and finds $\Delta \beta_e = 0.00453$ deg, which corresponds to the result of the simulations in Table 3, that is, $\Delta \beta_e = 0.00457$ deg. [The underlined digits in Table 3 represent the deviations of the analytical predictions in Eq. (21) relative to the simulated results]. In fact, the changes in the resulting attitude solutions are so small that the differences between the two methods have no practical relevance.

The second row in Table 3 uses biases of equal magnitudes (0.1 deg) but of opposite signs. This leads to a relatively large shift in the time of equal chords and a similarly large change in the resulting attitude solutions. The changes in the Earth aspect angle remain small, but the Earth reference direction will shift under the biases. The third and fourth rows provide the results for the individual bias errors on their own. The attitude errors in these cases are all of a similar magnitude and are about half as large as those in the second row. The attitude solutions in Table 3 were established by a geometric method, which includes the use of a “perfect” (i.e., without biases) sun–Earth dihedral-angle measurement α_e . If only the ϑ_e and β_e measurements were to be used, the changes in the attitude would be about 2.3 times as large in all cases shown here.

The final two rows in Table 3 summarize the effects of biases in the individual Earth radii. The propagation of a given bias $\Delta \rho_i$ into the chord measurement $\Delta \kappa_i$ (for any of the two chords $i = 1, 2$) at the time of equal chords can be established by means of the relevant partial derivative. Figure 5a shows that the equal-chord time is practically insensitive to uniform biases in the Earth radii. (The time of equal chords does shift slightly because the effects of the equal

$\Delta \rho_i$ biases on the two chords are not exactly equal.) In the case when the biases have opposite signs (Fig. 5b), there is a relatively large shift in the equal-chord time and also in the resulting attitude solutions.

In conclusion, we find that the worst-case magnitude of the attitude error is roughly equal to the root-sum-squared value of the individual biases in the two half-chord measurements. Both variants of the equal-chord method exhibit similar performances in terms of the resulting attitude errors. The approach using κ_e is perfectly insensitive to uniform biases in the Earth radii, whereas the approach using ρ_e is insensitive to uniform biases in the chord measurements. In the absence of a priori knowledge on the actual biases, we cannot express a meaningful preference for either of the two approaches.

V. Effects of Sensor Directional Biases

Another important error source affecting the attitude solution is caused by biases in the pointing directions of the Earth sensor pencil beams with respect to the actual in-flight spacecraft spin axis. These pointing errors are mainly caused by “dynamic imbalance,” which refers to the offset between the dynamical spin axis (along the axis of major or minor moment of inertia) and the designed spin axis, which is along the spacecraft geometrical centerline. In practice, we must account for uncertainty in the knowledge of the in-flight inertias caused by limitations in the precision of the balancing and by asymmetric fuel depletion. Furthermore, sensor mounting and internal misalignments can contribute (to a lesser degree) to the directional pointing bias.

We write $\mu_{i,\text{act}}$ for the actual (but unknown) mounting angles of the pencil beams relative to the actual in-flight spin axis, and we assume that the directional biases $\Delta \mu_i$ ($i = 1, 2$) are small:

$$\mu_{1,\text{act}} = \mu_1 + \Delta \mu_1, \quad \mu_{2,\text{act}} = \mu_2 + \Delta \mu_2 \quad (27)$$

The effects of the small biases $\Delta\mu_i$ on the attitude solution can be considered independent of those induced by the half-chord measurement biases just presented. Therefore, their respective contributions can be added in a first-order analysis, and it is meaningful to study the effects of the mounting biases in isolation here. The equal-chord condition under the actual mounting angles is formally identical to Eq. (7) but contains different “new” equal-chord parameters:

$$\kappa_{e,\text{new}} = \kappa_1(\beta_{e,\text{new}}, \rho_{e,\text{new}}, \mu_{1,\text{act}}) = \kappa_2(\beta_{e,\text{new}}, \rho_{e,\text{new}}, \mu_{2,\text{act}}) \quad (28)$$

After substituting the expressions of Eqs. (27) and expanding for small mounting biases $\Delta\mu_i$, we find first-order approximate expressions, which are identical in form to Eqs. (17):

$$\kappa_{e,\text{new}} \cong \kappa_1(\beta_{e,\text{new}}, \rho_{e,\text{new}}, \mu_1) + \Delta\kappa_1 \cong \kappa_2(\beta_{e,\text{new}}, \rho_{e,\text{new}}, \mu_2) + \Delta\kappa_2 \quad (29)$$

The expansion leading to Eq. (29) has transformed the directional biases $\Delta\mu_i$ into their corresponding biases in the individual chords $\Delta\kappa_i$ at the time of equal chords:

$$\Delta\kappa_i = \left(\frac{\partial\kappa_i}{\partial\mu_i} \right)_e \Delta\mu_i$$

with
$$\left(\frac{\partial\kappa_i}{\partial\mu_i} \right)_e = \frac{1}{(\tan\mu_i \tan\kappa_e)} - \frac{1}{(\tan\beta_e \sin\kappa_e)} \quad (30)$$

In the nominal CONTOUR case, the partials will be approximately ± 0.5 for the pencil beams 1 and 2, respectively.

At this stage we can reuse the model that was developed in Eqs. (17–26) to describe the effects of the measurement biases $\Delta\kappa_i$, that is,

$$\begin{aligned} \kappa_{e,\text{new}} &= \kappa_e + \Delta\kappa_e, & \rho_{e,\text{new}} &= \rho_e + \Delta\rho_e \\ \beta_{e,\text{new}} &= \beta_e + \Delta\beta_e \end{aligned} \quad (31)$$

The change in Earth aspect angle $\Delta\beta_e$ can be expressed in terms of $\Delta\rho_e$ or $\Delta\kappa_e$ as in Eqs. (21). Of particular interest is the result of Eq. (26), which expresses the changes in the equal-chord parameters $\Delta\kappa_e$ and Δt_e that are induced by the directional biases $\Delta\mu_i$ [via Eqs. (30)]:

$$\begin{aligned} \Delta\kappa_e &\cong 0.0901\Delta\mu_1 - 0.4024\Delta\mu_2 \text{ (deg)} \\ \Delta t_e &\cong -0.1250\Delta\mu_1 - 0.1194\Delta\mu_2 \text{ (h)} \end{aligned} \quad (32)$$

Table 4 summarizes the simulation results for the CONTOUR conditions. The first row shows that identical biases lead to an attitude change of a magnitude that is about half of the root-sum-squared value of the individual biases. The second row shows that biases with opposite signs lead to almost no change in the equal-chord time and have a negligible effect on the attitude solution. The attitude changes in the third and fourth rows are all of a similar magnitude and about half as large as those in the first row. If the geometric attitude determination were performed without the (perfect) measurements α_e , the attitude errors would be about 2.3 times as large.

VI. CONTOUR Flight Results

The equal-chord method was used³ for the attitude determination of CONTOUR in its spinning mode before the SRM firing on 15 August 2002. Table 5 shows the results for the attitude angles produced by the equal-chord method and the associated measurement residuals for the final six sensor coverage intervals. The “residuals” are the deviations between the actual equal-chord measurements and their predictions derived from simulations with the attitude solution produced by the method. We find that they are typically below 0.1 deg.

The beta column provides the results of both the baseline method (using the half-chord measurement κ_e) and the alternative approach (based on ρ_e). The differences between the two results are below 0.01 deg in all cases and as small as 0.004 deg in average. This indicates that the results of the two equal-chord approaches are very consistent. However, this does not necessarily imply that the resulting attitude error result will be low (because of unknown bias effects). The “goodness” column refers to the difference between the attitude determined from the sun and Earth angles ϑ_e and β_e and the solution that employs the dihedral angle α_e measurement in addition. The goodness angle reflects on the inherent consistency between the various measurement angles and can provide some indication on the presence of biases. Although the actual attitude direction is not known to sufficient precision to perform a persuasive comparison, we can conclude that the equal-chord method is capable of achieving an attitude-determination accuracy that is comparable to that of a more elaborate least-squares method (see also the results in Fig. 13 of Ref. 3).

Figure 6 illustrates the application of the quadratic approximations of the two sets of half-chord angles around the time of equal chords for CONTOUR’s Earth sensor data of 13 August 2002. The evolution of the residuals can be visualized as the discrepancy between the actual and predicted measurements.

Table 4 Effects of mounting misalignments on resulting attitude solution

Input biases	Changes in equal-chord parameters				Change in attitude	
	Δt_e , h	$\Delta\kappa_e$, deg	$\Delta\beta_e(\Delta\rho_e)$, deg	$\Delta\beta_e(\Delta\kappa_e)$, deg	$(\Delta\rho_e)$, deg	$(\Delta\kappa_e)$, deg
Identical: $\Delta\mu_1 = \Delta\mu_2 = 0.1$ deg	−0.02420	−0.03132	−0.00116	−0.00142	0.0718	0.0720
Opposite: $\Delta\mu_1 = -\Delta\mu_2 = 0.1$ deg	−0.00054	0.04807	−0.00003	0.00219	0.0016	0
Pencil beam # 1: $\Delta\mu_1 = 0.1$ deg; $\Delta\mu_2 = 0$	−0.01235	0.00869	−0.00059	0.00039	0.0367	0.0360
Pencil beam # 2: $\Delta\mu_1 = 0$; $\Delta\mu_2 = 0.1$ deg	−0.01180	−0.04064	−0.00057	−0.00184	0.0350	0.0360

Table 5 Summary of results and residuals (in degrees) of equal-chord method

Date	kappa	res (kap)	rho	res (rho)	beta		res (beta)	alpha	res (alpha)	theta	res (theta)	Goodness
					(rho)	(kap)						
15 Aug.	6.042	−0.175	6.086	0.018	62.864	62.856	−0.008	35.157	−0.072	103.043	−0.017	0.092
13 Aug.	6.129	−0.139	6.117	0.008	62.866	62.860	−0.006	36.662	−0.072	104.015	−0.025	0.092
11 Aug.	6.193	−0.085	6.133	0.015	62.867	62.862	−0.004	38.088	−0.063	104.946	−0.024	0.083
10 Aug.	6.126	−0.170	6.135	0.003	62.867	62.859	−0.007	39.539	−0.093	105.907	−0.014	0.087
8 Aug.	4.530	−0.006	4.734	−0.011	62.799	62.799	0.000	38.409	0.071	102.597	0.000	0.020
6 Aug.	4.620	0.054	4.771	0.004	62.800	62.802	0.002	39.520	−0.223	103.717	−0.042	0.214
Average	—	−0.087	—	−0.003	—	—	−0.004	—	−0.075	—	−0.020	0.117
Standard deviation	—	0.094	—	0.010	—	—	0.004	—	0.093	—	0.014	0.063

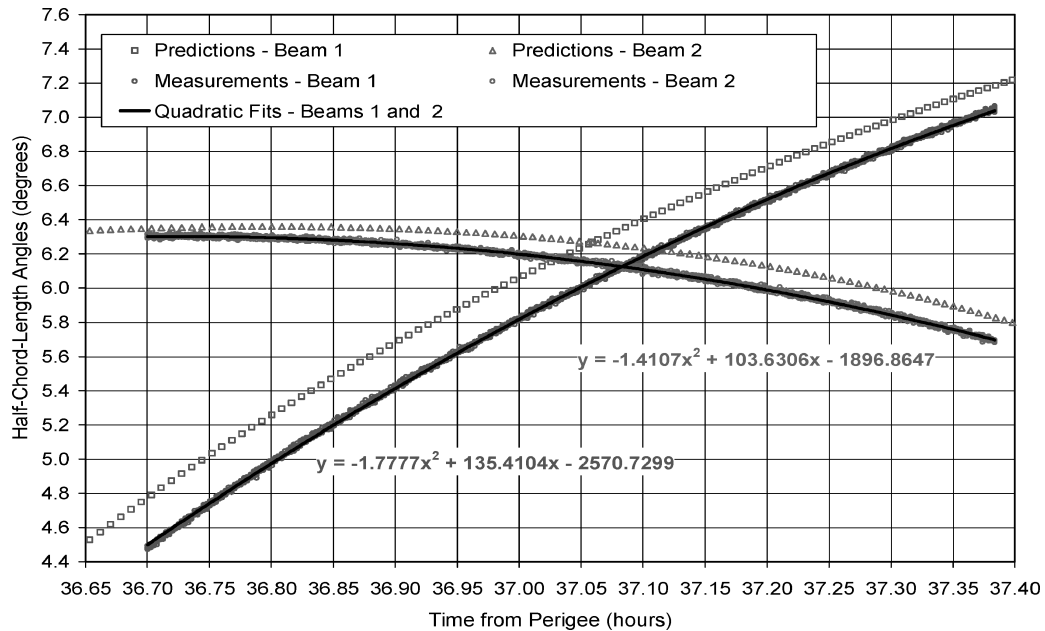


Fig. 6 Measured and predicted half-chord-length angles (13 Aug. 2002).

VII. Conclusions

We have presented a detailed outline of the principle and the operating procedure of the equal-chord method for spin-axis attitude determination. The method provides an attitude solution by using angular measurements referred to one single point during the Earth sensor coverage interval. This point corresponds to the instant when the chord lengths produced by the two pencil beams are equal and is determined by processing a set of about 1000 data points. The effects induced by the random noise in the sensor measurements can simply be removed by applying a linear (for the sun aspect and the sun–Earth dihedral angles) and a quadratic (for the chord angles) fitting procedure. The method does not require a priori attitude knowledge, but a rough idea of the time of equal chords is needed to identify the interval of data for processing. We demonstrate that the resulting attitude solution is practically insensitive to uniform biases in the measured chord lengths at the time of equal chords. These biases can be induced for instance by local variations in the radiance profile of the Earth’s infrared radius. Furthermore, the influence of sensor directional biases on the attitude solution produced by the equal-chord method has been analyzed. The results demonstrate that the equal-chord method offers an efficient, robust, straightforward, and low-cost alternative to the more traditional attitude estimation methods.

References

- ¹Farquhar, R. W., and Dunham, D., “The Indirect Launch Mode: A New Launch Technique for Interplanetary Missions,” International Academy of Astronautics, Paper L98-0901, May 1998.
- ²Muhonen, D. P., Farquhar, R. W., Holdridge, M., and Reynolds, E., “Design and Implementation of CONTOUR’s Phasing Orbits,” AAS Paper 03-208, Feb. 2003.
- ³van der Ha, J., Rogers, G., Dellinger, W., and Stratton, J., “CONTOUR Phasing Orbits: Attitude Determination & Control Concepts and Flight Results,” AAS Paper 03-150, Feb. 2003.
- ⁴van der Ha, J. C., “Spin Axis Attitude Determination Accuracy Model,” International Astronautical Congress, Paper IAC-03-A.5.08, Sept.–Oct. 2003.
- ⁵Wertz, J. R. (ed.), *Spacecraft Attitude Determination and Control*, Reidel, Dordrecht, The Netherlands, 1978, Chaps. 10–14.
- ⁶Fagg, A. S., and van Holtz, L., “Application of Simplified Spin Axis Attitude Determination Techniques to ESA Telecom Satellites,” *Proceedings of the CNES Symposium on “Space Dynamics for Geostationary Satellites,”* edited by J.-P. Carrou, Cepadues Editions, Toulouse, France, 1985, pp. 219–226.
- ⁷van der Ha, J. C., “Attitude Determination Covariance Analysis for Geostationary Transfer Orbits,” *Journal of Guidance, Control, and Dynamics*, Vol. 9, No. 2, 1986, pp. 156–163.
- ⁸Shuster, M. D., “Efficient Algorithms for Spin-Axis Attitude Estimation,” *Journal of the Astronautical Sciences*, Vol. 31, No. 2, 1983, pp. 237–249.